



ELSEVIER

Contents lists available at ScienceDirect

## Measurement

journal homepage: [www.elsevier.com/locate/measurement](http://www.elsevier.com/locate/measurement)

## An accelerometer for spaceborne application with interferometric readout

Marco Pisani<sup>1</sup>, Massimo Zucco<sup>1,\*</sup>

Istituto Nazionale di Ricerca Metrologica, INRIM, Torino, Italy

## ARTICLE INFO

## Keywords:

Laser interferometer  
Accelerometer

## ABSTRACT

Accelerometers for space applications are typically based on a capacitive readout. Here we present the design of an accelerometer based on a classical mass spring mechanical system with an interferometric readout. The heterodyne interferometer is completely fiber based with a 1064 nm diode laser source and has a subpicometer resolution at 1 Hz. We present and discuss the design and the characterization of the interferometer, the foreseen performances of the whole accelerometer and the characterization strategies of the same.

## 1. Introduction

Acceleration measurements are needed to various levels of sensitivity for almost all space missions in the fields of fundamental physics, space geodesy, space exploration, as well as on space stations. Acceleration sensors have a “free” (or weakly coupled) test mass inside a cage rigid with the spacecraft, and yield their relative acceleration by reading the relative displacements (linear and angular, if needed) of the test mass with respect to the cage. The accelerations of interest require very low noise readout also at low frequencies. Typically, the displacement measurement is made with a capacitive sensor with a first armature fixed to the cage, the second one being the mass itself, which is made of, or properly coated with metal [1–3].

Laser interferometers have demonstrated to be able to measure displacements with accuracies to the level of the picometer [4] and their use is foreseen in high-resolution measurement in space [5]. Today's laser sources -such as solid state diode pumped lasers, extended cavity diode lasers or fiber lasers- can be integrated in compact subsystems suitable for space missions. In addition, a plethora of fiber integrated components (mostly coming from telecom industry) allow us to realize compact and robust interferometers which could be used in the next future in place of capacitive sensors.

Laser interferometry readout has two advantages with respect to capacitive readout. In the first place, the laser interferometer output is linear with the gap  $D$  between the test mass and the cage, while it is known that capacitive sensors readout can be linearized only for very small changes in  $D$ . Secondly the sensitivity of the interferometer readout is independent of the gap  $D$ , while in a capacitive sensor it goes as  $1/D$ , which leads to use narrow gaps and therefore to face the related noise sources (e.g. the noise due to residual pressure is larger for

narrower gaps). Furthermore, if low frequency thermo-mechanical drifts (i.e. “real” drifts) are properly taken care of, there is no increase of noise due to the laser interferometer at low frequencies.

We report on the design of an accelerometer equipped with an interferometric readout expressly planned for scientific missions where very small accelerations have to be accurately measured. The interferometer is based on an all-fiber heterodyne at  $\lambda \approx 1064$  nm.

## 2. The accelerometer

The accelerometer we have designed to demonstrate the feasibility of the interferometric readout is based on a simple mass spring assembly taken from an accelerometer realized by IAPS-CNR. The dual axes accelerometer, called ISA-GGG, was intended to monitor the environmental seismic vibrations of the laboratory and is described in [6]. The mass and the spring are machined from the same aluminum block. The principle of the accelerometer is based on a test mass  $m$  attached to the cage through the spring with stiffness  $k$ , cfr Fig. 1. The spring is in fact a thin vertical foil, which allows the mass to move horizontally while keeping it constrained in the vertical axis, as represented in Fig. 9. A damping coefficient  $\zeta$ , however small, is always present.

The equation of motion of the damped spring is a second order linear differential equation with constant coefficients, where  $ma(t)$  is the force applied to the test mass  $m$  through the acceleration  $a(t)$ .

$$m\ddot{x} + k\dot{x} + \zeta x = ma(t) \quad (1)$$

The resonant frequency is given by  $\omega_0 = \sqrt{\frac{k}{m}}$ , which in our case is  $\omega_0 = 18.8$  rad/s, or equivalently  $f_0 \approx 3$  Hz. For excitation frequencies below resonance, and for steady state, the displacement  $x$  is given by:

\* Corresponding author.

E-mail addresses: [m.pisani@inrim.it](mailto:m.pisani@inrim.it) (M. Pisani), [m.zucco@inrim.it](mailto:m.zucco@inrim.it) (M. Zucco).<sup>1</sup> These authors contributed equally to this work.

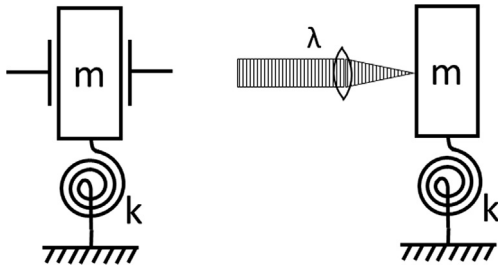


Fig. 1. Left: the classical accelerometer with mass spring assembly and capacitive readout of the displacement. The sensitivity in acceleration is limited by the noise limit of the displacement sensor. Right: the same accelerometer equipped where the displacement of the test mass is measured by an interferometric readout system. The noise of the interferometer can be lower than the capacitive sensor, in particular at large distance between the armatures.

$$x = \frac{m}{k}a = \frac{a}{\omega_0^2} \quad (2)$$

The sensitivity  $S$  of the accelerometer is given by the ratio  $x/a$  giving  $S = \frac{x}{a} = \frac{1}{\omega_0^2}$ , therefore the sensitivity  $S$  is inversely proportional to the spring constant  $k$ . This accelerometer ISA-GGG makes use of a pair of electrodes to read the displacement of the mass and a second pair of electrodes to reduce the spring constant  $k$  (increasing the sensitivity) and to move the mass for calibration purposes. In our sensor, the electrodes for the capacitive readout are not used and the mass and the cage will be modified to host the mirrors of the interferometer. The sensitivity  $S$  of the accelerometer for high frequency, above the resonant frequency, is independent of the accelerometer parameters and depends only on the angular frequency:

$$S(\omega) = \frac{1}{\omega^2} \quad (3)$$

The actuator electrodes will be kept operative for their original purpose, i.e. for in flight calibration and/or for reducing the natural resonant frequency. The same mass spring set-up has been adopted for the three ISA accelerometers of the BepiColombo mission.

### 3. The interferometer

A schematic diagram of the interferometer readout (here called Laser Interferometry Gauge, LIG) is shown in Fig. 2 where the opto-electronics board contains the readout instrumentation connected through PM fibers to the optical head. The laser source is a continuous-

wave high performance Planar-Waveguide External Cavity Diode Laser (PW-ECL) from Redfern Integrated Optics (RIO) working at wavelength  $\lambda = 1064$  nm. This wavelength was chosen because is in coincidence with the emission of Nd:YAG lasers, considered as a standard in the space application and it is used in Lisa pathfinder [7], GRACE Follow-on [8]. The low phase noise of the lasers based on PW-ECL showed that they are good candidates for interferometric applications [9]. Consequently, various opto-electronic and optical components have been space qualified and used in space. In the scheme, the laser output is directly coupled into a PM fiber and is split in two parts, which undergo differential frequency shifts by means of two acousto-optic modulators (AOM) at frequencies  $\nu_2$  and  $\nu_1$ . The frequency difference is the heterodyne frequency  $f_{het} = \nu_2 - \nu_1$ . Then the two radiations are sent through PM fibers to the optical head where a classical polarization separation Michelson interferometer is used to measure the relative displacement between the two mirrors M1 and M2. One of the mirrors will be used as a fixed reference and the other will be fixed to the moving test mass. The mirrors can be indifferently flat mirrors or corner cube retroreflectors (CCR). In our preferred realization, the mirror fixed to the test mass will be a CCR in order to guarantee the self-alignment of the interferometer. The reference signal of the heterodyne interferometer is generated by superposing and making interfere the two radiations spilled from the polarization beam splitter PBS before entering in the interferometer. The interfering beam is sent back through the fiber to the detector on the opto-electronic board. Regarding the measurement signal, the second PBS separates the radiations to be sent to the two mirrors M1 and M2 and recombines them in the interfering beam sent to the “measurement” detector on the optical board through the PM fiber. Two half-wave plates at the exit of the fiber launchers are used to change the power of the beam after the PBS in order to maximize the visibility of the heterodyne signals.

In Fig. 3 is shown a picture of the optical part of the LIG prototype. The optical components are glued to a zerodur base. The power of the laser beams reflected on the test masses is kept as low as  $1 \mu\text{W}$  in order to have a negligible effect due to the radiation pressure on the displacement of the masses and a negligible heating of the mass. This power level, on the other hand, is high enough to guarantee a signal to noise ratio,  $\text{SNR} > 10^6$  in the band of 1 Hz, to the interferometric signal allowing a resolution better than  $1 \text{ pm}/\sqrt{\text{Hz}}$  on the displacement PSD.

The two electric signals at  $f_{het}$  coming from the two detectors are sent to an A/D converter and elaborated via a LabView® software that implements the IQ demodulation and calculates the phase  $\Delta\phi$  between the two signals, hence the relative displacement between the two test

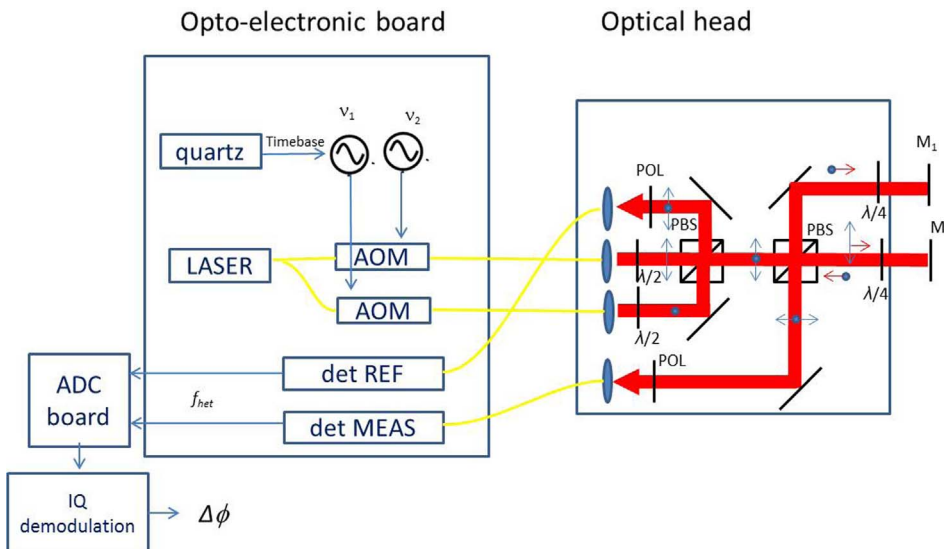


Fig. 2. Schematic of the LIG. The three units are: the opto-electronic board where the instrumentation is present, the optical head with the optical components and the electronics to measure the phase difference. The yellow lines are optical fibers, the red lines the radiations and the blue lines the electric signals. (For interpretation of the references to colour in this figure legend, the reader is referred to the web version of this article.)

Download English Version:

<https://daneshyari.com/en/article/7121749>

Download Persian Version:

<https://daneshyari.com/article/7121749>

[Daneshyari.com](https://daneshyari.com)